



## Research Article

M.C. Montesi, A. Lauria\*, A. Alexandrov, L. Alunni Solestizi, Ambrosi Giovanni, S. Argirò, R. Arteché Diaz, N. Bartosik, G. Battistoni, N. Belcari, E. Bellinzona, S. Bianucci, S. Biondi, M.G. Bisogni, G. Bruni, N. Camarlinghi, P. Carra, P. Cerello, E. Ciarrocchi, A. Clozza, S. Colombi, A. Del Guerra, M. De Simoni, A. Di Crescenzo, M. Donetti, Y. Dong, M. Durante, A. Embriaco, M. Emde, R. Faccini, V. Ferrero, F. Ferroni, E. Fiandrini, C. Finck, E. Fiorina, M. Fischetti, M. Francesconi, M. Franchini, G. Galati, L. Galli, M. Garbini, V. Gentile, G. Giraudo, R. Hetzel, E. Iarocci, M. Ionica, K. Kanxheri, A. C. Kraan, V. Lante, C. La Tessa, E. Lopez Torres, M. Marafini, I. Mattei, A. Mengarelli, R. Mirabelli, A. Moggi, M.C. Morone, M. Morrocchi, S. Muraro, L. Narici, A. Pastore, N. Pastrone, V. Patera, F. Pennazio, P. Placidi, M. Pullia, F. Raffaelli, L. Ramello, R. Ridolfi, V. Rosso, M. Rovituso, C. Sanelli, A. Sarti, G. Sartorelli, O. Sato, S. Savazzi, L. Scavarda, A. Schiavi, C. Schuy, E. Scifoni, A. Sciubba, A. Sécher, M. Selvi, L. Servoli, G. Silvestre, M. Sitta, R. Spighi, E. Spiriti, G. Sportelli, A. Stahl, V. Tioukov, S. Tomassini, F. Tommasino, G. Traini, S.M. Valle, M. Vanstalle, M. Villa, U. Weber, A. Zoccoli, and G. De Lellis

# Ion charge separation with new generation of nuclear emulsion films

<https://doi.org/10.1515/phys-2019-0024>

Received Dec 12, 2018; accepted Feb 06, 2019

**\*Corresponding Author: A. Lauria:** University of Napoli, Department of Physics "E. Pancini", Napoli, Italy; Istituto Nazionale di Fisica Nucleare (INFN), Section of Napoli, Napoli, Italy; Email: [adele.lauria@unina.it](mailto:adele.lauria@unina.it)

**M.C. Montesi, A. Di Crescenzo:** University of Napoli, Department of Physics "E. Pancini", Napoli, Italy; Istituto Nazionale di Fisica Nucleare (INFN), Section of Napoli, Napoli, Italy

**A. Alexandrov:** University of Napoli, Department of Physics "E. Pancini", Napoli, Italy; Istituto Nazionale di Fisica Nucleare (INFN), Section of Napoli, Napoli, Italy; National University of Science and Technology MISIS, RUS-119049; Lebedev Physical Institute of the Russian Academy of Sciences, RUS-119991 Moscow, Russia

**L. Alunni Solestizi, E. Fiandrini, G. Silvestre:** Istituto Nazionale di Fisica Nucleare (INFN), Section of Perugia, Perugia, Italy; University of Perugia, Department of Physics and Geology, Perugia, Italy

**Ambrosi Giovanni, M. Ionica, K. Kanxheri, L. Servoli:** Istituto Nazionale di Fisica Nucleare (INFN), Section of Perugia, Perugia, Italy

**S. Argirò, V. Ferrero, L. Scavarda:** University of Torino, Department of Physics, Torino, Italy; Istituto Nazionale di Fisica Nucleare (INFN), Section of Torino, Torino, Italy

**R. Arteché Diaz:** CEADEN, Centro de Aplicaciones Tecnológicas y Desarrollo Nuclear, Havana, Cuba

**N. Bartosik, P. Cerello, G. Giraudo:** Istituto Nazionale di Fisica Nucleare (INFN), Section of Torino, Torino, Italy

**G. Battistoni, A. Embriaco, I. Mattei:** Istituto Nazionale di Fisica Nucleare (INFN), Section of Milano, Milano, Italy

**N. Belcari, M.G. Bisogni, N. Camarlinghi, P. Carra, E. Ciarrocchi, A. Del Guerra, M. Francesconi, M. Morrocchi, V. Rosso, G. Sportelli:** University of Pisa, Department of Physics, Pisa, Italy;

Istituto Nazionale di Fisica Nucleare (INFN), Section of Pisa, Pisa, Italy

**E. Bellinzona, M. Rovituso, E. Scifoni:** Trento Institute for Fundamental Physics and Applications, Istituto Nazionale di Fisica Nucleare (TIFPA-INFN), Trento, Italy

**S. Bianucci, L. Galli, A. C. Kraan:** Istituto Nazionale di Fisica Nucleare (INFN), Section of Pisa, Pisa, Italy

**S. Biondi, M. Franchini, G. Sartorelli, M. Villa, A. Zoccoli:** Istituto Nazionale di Fisica Nucleare (INFN), Section of Bologna, Bologna, Italy; University of Bologna, Department of Physics and Astronomy, Bologna, Italy

**G. Bruni, A. Mengarelli, M. Selvi, R. Spighi:** Istituto Nazionale di Fisica Nucleare (INFN), Section of Bologna, Bologna, Italy

**N. Bartosik, P. Cerello, G. Giraudo:** Istituto Nazionale di Fisica Nucleare (INFN), Section of Torino, Torino, Italy

**A. Clozza, E. Iarocci, C. Sanelli, E. Spiriti, S. Tomassini:** Istituto Nazionale di Fisica Nucleare (INFN), Laboratori Nazionali di Frascati, Frascati, Italy

**S. Colombi, C. La Tessa, F. Tommasino:** Trento Institute for Fundamental Physics and Applications, Istituto Nazionale di Fisica Nucleare (TIFPA-INFN), Trento, Italy; University of Trento, Department of Physics, Trento, Italy

**M. De Simoni, R. Faccini, F. Ferroni:** University of Rome La Sapienza, Department of Physics, Rome, Italy; Istituto Nazionale di Fisica Nucleare (INFN), Section of Roma 1, Rome, Italy

**M. Donetti:** Istituto Nazionale di Fisica Nucleare (INFN), Section of Torino, Torino, Italy; Centro Nazionale di Adroterapia Oncologica (CNAO), Pavia, Italy

**Y. Dong, S.M. Valle:** Istituto Nazionale di Fisica Nucleare (INFN), Section of Milano, Milano, Italy; University of Milano, Department of Physics, Milano, Italy

**Abstract:** In hadron therapy, the accelerated ions, interacting with the body of the patient, cause the fragmentation of both projectile and target nuclei. The fragments interact with the human tissues depositing energy both in the entrance channel and in the volume surrounding the tumor. The knowledge of the fragments features is crucial to de-

termine the energy amount deposited in the human body, and - hence - the damage to the organs and to the tissues around the tumor target.

The FOOT (FragmentatiON Of Target) experiment aims at studying the fragmentation induced by the interaction of a proton beam (150-250 MeV/n) inside the human body. The FOOT detector includes an electronic setup for the identification of  $Z \geq 3$  fragments integrated with an emulsion spectrometer to measure  $Z \leq 3$  fragments. Charge identification by nuclear emulsions is based on the development of techniques of controlled fading of the particle tracks inside the nuclear emulsion, that extend the dynamical range of the films developed for the tracking of minimum ionising particles. The controlled fading strongly depends on temperature, relative humidity and treatment duration.

In this study the performances in terms of charge separation of proton, helium and carbon particles, obtained on a batch of new emulsion films produced in Japan are reported.

**Keywords:** Charge identification, nuclear emulsions, charged particles therapy

**PACS:** 29.40.Rg, 42.62.Be

**M. Durante:** Biophysics Department, GSI Helmholtzzentrum für Schwerionenforschung, Darmstadt, Germany; Technische Universität Darmstadt Institut für Festkörperphysik, Darmstadt - Germany

**M. Emde, R. Hetzel, A. Stahl:** RWTH Aachen University, Physics Institute III B, Aachen, Germany

**C. Finck, A. Sécher, M. Vanstalle:** Université de Strasbourg, CNRS, IPHC UMR 7871, F-67000 Strasbourg, France

**E. Fiorina:** Istituto Nazionale di Fisica Nucleare (INFN), Section of Pisa, Pisa, Italy; Centro Nazionale di Adroterapia Oncologica (CNAO), Pavia, Italy

**M. Fischetti:** University of Rome La Sapienza, Department of Scienze di Base e Applicate per l'Ingegneria (SBAI), Rome, Italy; Istituto Nazionale di Fisica Nucleare (INFN), Section of Roma 1, Rome, Italy

**G. Galati, V. Tioukov:** Istituto Nazionale di Fisica Nucleare (INFN), Section of Napoli, Napoli, Italy

**M. Garbini:** Istituto Nazionale di Fisica Nucleare (INFN), Section of Bologna, Bologna, Italy; University of Bologna, Department of Physics and Astronomy, Bologna, Italy; Museo Storico della Fisica e Centro Studi e Ricerche Enrico Fermi, Rome, Italy

**V. Gentile:** Gran Sasso Science Institute, L'Aquila, Italy

**V. Lante, M. Pullia, S. Savazzi:** Centro Nazionale di Adroterapia Oncologica (CNAO), Pavia, Italy

**E. Lopez Torres:** Istituto Nazionale di Fisica Nucleare (INFN), Section of Torino, Torino, Italy; CEADEN, Centro de Aplicaciones Tecnológicas y Desarrollo Nuclear, Havana, Cuba

**M. Marafini:** Istituto Nazionale di Fisica Nucleare (INFN), Section of Roma 1, Rome, Italy; Museo Storico della Fisica e Centro Studi e Ricerche Enrico Fermi, Rome, Italy

**R. Mirabelli, G. Traini:** University of Rome La Sapienza, Department of Physics, Rome, Italy; Istituto Nazionale di Fisica Nucleare (INFN), Section of Roma 1, Rome, Italy; Museo Storico della Fisica e Centro Studi e Ricerche Enrico Fermi, Rome, Italy

**A. Moggi, S. Muraro, F. Raffaelli:** University of Pisa, Department of Physics, Pisa, Italy

**M.C. Morone, L. Narici:** University of Rome Tor Vergata, Department of Physics, Rome, Italy; Istituto Nazionale di Fisica Nucleare (INFN), Section of Roma Tor Vergata, Rome, Italy

**A. Pastore:** Istituto Nazionale di Fisica Nucleare (INFN), Section of Bari, Bari, Italy

**N. Pastrone, F. Pennazio:** University of Torino, Department of Physics, Torino, Italy

**V. Patera:** University of Rome La Sapienza, Department of Physics, Rome, Italy; University of Rome La Sapienza, Department of Scienze di Base e Applicate per l'Ingegneria (SBAI), Rome, Italy; Museo Storico della Fisica e Centro Studi e Ricerche Enrico Fermi, Rome, Italy

**P. Placidi:** Istituto Nazionale di Fisica Nucleare (INFN), Section of Perugia, Perugia, Italy; University of Perugia, Department of Engineering, Perugia, Italy

**L. Ramello, M. Sitta:** University of Torino, Department of Physics, Torino, Italy; University of Piemonte Orientale, Department of Science and Technological Innovation, Alessandria, Italy

**R. Ridolfi:** University of Bologna, Department of Physics and Astronomy, Bologna, Italy

**A. Sarti:** Istituto Nazionale di Fisica Nucleare (INFN), Laboratori Nazionali di Frascati, Frascati, Italy; University of Rome La Sapienza, Department of Scienze di Base e Applicate per l'Ingegneria (SBAI), Rome, Italy; Museo Storico della Fisica e Centro Studi e Ricerche Enrico Fermi, Rome, Italy

**O. Sato:** Nagoya University, Department of Physics, Nagoya, Japan

**A. Schiavi:** Istituto Nazionale di Fisica Nucleare (INFN), Section of Roma 1, Rome, Italy; University of Rome La Sapienza, Department of Scienze di Base e Applicate per l'Ingegneria (SBAI), Rome, Italy

**C. Schuy, U. Weber:** Biophysics Department, GSI Helmholtzzentrum für Schwerionenforschung, Darmstadt, Germany

**A. Sciubba:** Istituto Nazionale di Fisica Nucleare (INFN), Section of Roma 1, Rome, Italy; University of Rome La Sapienza, Department of Scienze di Base e Applicate per l'Ingegneria (SBAI), Rome, Italy; Museo Storico della Fisica e Centro Studi e Ricerche Enrico Fermi, Rome, Italy

**G. De Lellis:** University of Napoli, Department of Physics "E. Pancini", Napoli, Italy; Istituto Nazionale di Fisica Nucleare (INFN), Section of Napoli, Napoli, Italy; CERN

## 1 Introduction

Charged Particles Therapy (CPT) is an established therapy for the cancer treatment. Advantages of CPT with respect to the traditional X-rays therapy are due to their different ways to release energy passing through the human tissues. X-rays release energy along the whole path, while hadrons deliver most of their energy at the end of their path, in the Bragg peak [1]. In addition to that, hadron beams are characterised by an enhanced biological effectiveness. This is evaluated in terms of the Relative Biological Effectiveness (RBE), defined as the ratio of photon to charged particle dose producing the same biological effect. RBE value for protons is assessed around to 1.1 [2]. Recent radiobiological studies for proton beams show a considerable variation of this value (up to 1.7), in the volume surrounding the tumor [3], depending on many factors (dose, biological endpoints, Linear Energy Transfer, organs, patients variability). Different studies indicate that a significant contribution to the dose deposition is due to the nuclear fragmentation of the target nuclei of the human body [4], especially in the healthy tissues along the entrance channel [5]. Further investigations in order to better understand the dose contribution due to secondary fragments in healthy tissues is a relevant topic [6]. Very limited data are available in literature due to the complexity of dedicated experiments to be performed. Fragments produced by nuclear fragmentation of the target have low kinetic energy and thus sub-mm range confined in the target.

The FOOT experiment will study the target fragmentation induced by 150-250 MeV proton beams on human tissues through the inverse kinematic approach. It consists to invert the role of the beam and of the target with a Lorentz transformation measuring the cross sections of  $^{12}\text{C}$  and  $^{16}\text{O}$  that interact (with the same energy per nucleon) with a proton target. Instead of adopting an inconvenient low-density gaseous proton target, FOOT will take data with two different targets, a pure carbon (graphite) and a hydrogen enriched ( $\text{C}_2\text{H}_4$ ) target [7]. The cross-section of  $^{12}\text{C}$  and  $^{16}\text{O}$  interactions with hydrogen are then obtained by a linear combination of the above measurements. The aim of the experiment is to measure the fragment production cross section with uncertainty better than 5% and the energy spectra with a resolution of about 1-2 MeV/n in the inverse kinematic frame. Moreover, it is designed to identify the charge of fragments with an accuracy of 2-3%, and to perform an isotopic identification up to 5%.

The FOOT detector consists of two different setup. The first one is made of a magnetic spectrometer, based on pixel and microstrip detectors (for momentum reconstruction),

a plastic scintillator (to measure the energy loss  $dE/dx$  and the Time Of Flight (TOF)) and a calorimeter (to measure the kinetic energy) [8]. This electronic setup aims at measuring heavier fragments with  $Z \geq 3$  and covers a polar angle inside  $\pm 10^\circ$  with respect to the beam axis. Complementary to the electronic detector, a setup based on an emulsion spectrometer is used for the measurements of light fragments emitted at an angle up to about  $70^\circ$ .

The identification of different charged particles was already achieved with the Emulsion Cloud Chamber (ECC) technique with OPERA-like films [9–11]. Nuclear emulsions allow the measurement of particle trajectories (emitted up to  $80^\circ$  [12]) with sub-micrometer spatial resolution [13]. It was demonstrated that a controlled fading of the emulsions in terms of different thermal treatments extends their response to a broader range, becoming sensitive to different charges [9].

The data presented in this work were obtained exposing nuclear emulsions to different beam nuclei such as protons, helium and carbons, at the kinetic energy of 80 MeV/n at Laboratori Nazionali del Sud (LNS, Catania, Italy). The aim of this work was to determine the optimal thermal treatment to separate protons from MIP (Minimum Ionizing Particles) and helium from protons and carbon ions with newly produced emulsion films.

## 2 Nuclear emulsions

A nuclear emulsion film (shown in Figure 1) consists of two  $80 \mu\text{m}$  thick sensitive emulsion layers (made of a gel with interspersed AgBr crystals and called top and bottom layers, respectively) deposited on both sides of a plastic base,  $180 \mu\text{m}$  thick. These films were produced at Nagoya University in June 2017 and are different from those produced in

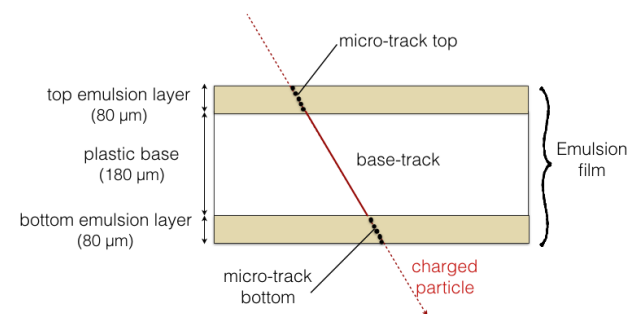


**Figure 1:** Scheme of a nuclear emulsion film of new generation. A sequence of aligned clusters in top and bottom layers of the emulsion form micro-tracks. Aligned top and bottom micro-tracks form base-tracks.

the OPERA experiment, hence the need for their characterisation in terms of controlled fading.

The passage of a charged particle through a nuclear emulsion impresses silver grains along its path giving raise to a latent image that after chemical process produces a chain of black silver grains. The silver grains along the particle trajectory are reconstructed by a fully automated optical microscope with sub-micrometric accuracy as clusters of pixels above threshold after the digitization of the grabbed images [14, 15]. A dedicated software recognizes aligned clusters of pixels on the two different emulsion layers producing a micro-track [16].

Two aligned micro-tracks in the two emulsion layers form a base-track. A sequence of aligned base-tracks in adjacent films defines a volume track. From the density of silver grains along the trajectory it is possible to measure the ionization of the incident particle. The reconstructed base-track has a micrometer accuracy of  $0.3 \mu\text{m}$  in position and  $1.2 \text{ mrad}$  in angle [17].

The films were stored at  $4^\circ\text{C}$  except during the exposure time. The sensitivity of these emulsion films, for particles at minimum of their ionizing power (MIP) observed as thin tracks, is about 50 grains/100  $\mu\text{m}$  (higher than the OPERA films, 30 grains/100  $\mu\text{m}$ ) [11].

The grain density is proportional to the energy loss by primary ionization. For highly ionizing particles, a saturation effect occurs due to the limited range of the grain density, thus preventing the charge measurement. As an example, the image of a field of view taken at the optical microscope, showing the interaction of a carbon ion (left) and a proton (right), impinging perpendicularly to the emulsion surface, is reported Figure 2. While the proton particle appears as a single spot of few black pixels, the carbon one appears as larger black spot with several delta-rays nearby.

It is possible to extend the dynamical range of the emulsion response to heavier ( $Z > 1$ ) particles by keeping the

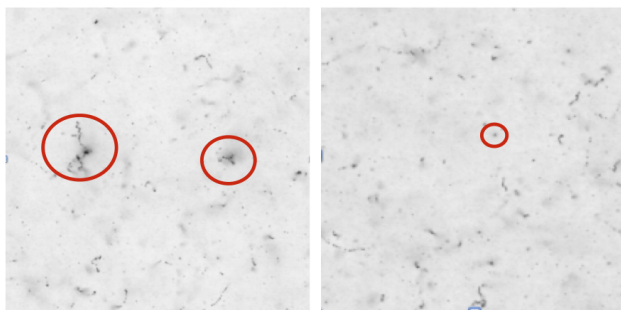


**Figure 2:** Tracks in emulsion generated by passing through carbons (left) and protons (right) impinging perpendicularly to the emulsion surface. In the left image delta rays emitted from the carbon interaction are also visible. View size is  $300 \times 300 \mu\text{m}^2$ .

emulsions for 24 hours for each treatment at a relatively high temperature (above  $28^\circ\text{C}$ ) and a high relative humidity (around 98%): a controlled fading is induced in order to partially or totally erase the tracks of the less ionizing particles [20], i.e. reducing the number of black pixels associated to the cluster. This thermal treatment was applied with the aim to optimize the temperature values for the new batch of films to be used in the framework of the FOOT experiment.

## 3 Methods

### 3.1 Film exposure and treatment

We assembled 40 emulsion films were assembled two by two (i.e. 20 doublets) under vacuum in the Emulsion Laboratory in Napoli, with a  $100 \mu\text{m}$  thick and light-tight aluminum paper. The film surface has a size of  $5.0 \times 4.0 \text{ cm}^2$ . The doublets were exposed at LNS to H,  $^2\text{H}$ ,  $^4\text{He}$  and  $^{12}\text{C}$  particles beam at 80 MeV/n (five doublets for each particle beam). The exposure setup is shown in Figure 3. The beam flux and the beam spot size were set in a control room and they were monitored soon before the emulsion exposure by a silicon microstrip detector and by a CMOS sensor in the experimental room.

The emulsion surface was placed perpendicularly to the beam direction and the integrated flux was about  $1000 \text{ nuclei/cm}^2$ , statistically sufficient for the purposes of presented study.

After the exposures the emulsions were carried to the

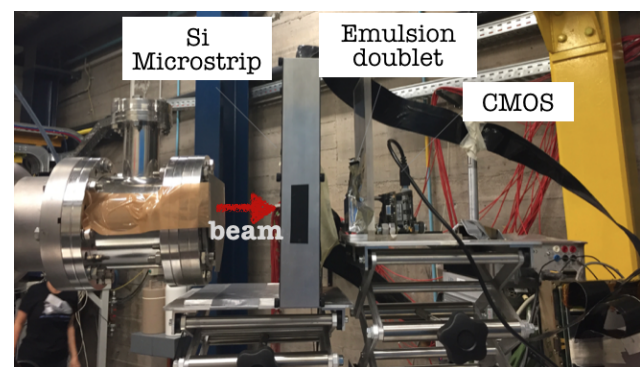


**Figure 3:** Scheme of the setup emulsion exposure at LNS.

Laboratori Nazionali del Gran Sasso (LNGS, Assergi - AQ) where thermal treatments (called refreshing, in the following indicated as R) were applied in a dedicated facility. All the films were treated at the relative humidity of



98%, at the following temperatures:  $T=28^{\circ}\text{C}$  (R1),  $T=34^{\circ}\text{C}$  (R2),  $T=36^{\circ}\text{C}$  (R3) and  $T=38^{\circ}\text{C}$  (R4). In Table 1, beam exposures and thermal treatments are summarized. A label  $Rn$  is given to each doublet.

**Table 1:** Scheme of emulsion exposures and thermal treatment conditions. Emulsion doublets were exposed at LNS (July 2017). All the thermal treatments and the developments were performed at LNGS.

Beam particle	Beam Energy (MeV)	Treatment Temperature ( $^{\circ}\text{C}$ )	Thermal ID
H	80	no treatment	R0
		28	R1
		34	R2
		36	R3
		38	R4
$^2\text{H}$	80	no treatment	R0
		28	R1
		34	R2
		36	R3
		38	R4
$^4\text{He}$	80	no treatment	R0
		28	R1
		34	R2
		36	R3
		38	R4
$^{12}\text{C}$	80	no treatment	R0
		28	R1
		34	R2
		36	R3
		38	R4

### 3.2 Analysis

After the thermal treatment, emulsions were chemically developed at LNGS and then brought to the Emulsion Laboratory in Napoli, where they were analyzed by fast automated microscopes operating at high speed (up to  $190\text{ cm}^2/\text{hour}$ ) with tracking efficiency larger than 90% [17]. The automated system consists of a microscope equipped with a 3D motorized translation stage, a dedicated optical system and a CCD camera. The digitalization process converts aligned grains ( $\sim 40$  grains in each emulsion layer for a MIP) in the particle track. The sum of all the pixels corresponding to the particle track is proportional, as the grain density, to the specific ionization, and hence to the square

of the charge particle.

This sum (track volume) is the parameter we use for the charge separation of incident particles: it is measured in terms of number of pixels [16]. This parameter changes as a function of the treatment temperature, therefore it can be distinguish different ionizing particles (such as MIP, H,  $^4\text{He}$  and  $^{12}\text{C}$ ) by an appropriate combination of the track volumes. Thermal treatment partially or totally erases the tracks of particles, according to the temperature values, thus mitigating the saturation effect. So, the track volumes (VR0, VR1, VR2, VR3 and VR4) for each thermal treatment (R0, R1, R2, R3 and R4, respectively) were measured. The track volumes were normalized with respect to the emulsion thickness.

The dedicated software, acquiring clusters of pixels, separates through a digital filtration process the background contribution (accidental specks) from the signal (cosmic rays and ionizing beam particles). Clusters are made of pixels. The operation to produce clusters passes through a filtering algorithm consisting of a matrix operation over each pixel value:

$$g_{ij} = \text{Tr} F^T C_{ij}$$

where  $g_{ij}$  is the new pixel value ( $i, j$ ),  $\text{Tr} F$  is the trace of the filter matrix and  $^T C_{ij}$  is the transposed matrix of the  $C_{ij}$  matrix.  $C_{ij}$  is composed of the pixel value ( $i, j$ ) and the values of the surrounding pixels such that the value  $g_{ij}$  of the pixel ( $i, j$ ) is the central element of the matrix  $C_{ij}$  [19]. The size and the values of the matrix  $F$  must be optimized according to the size of the cluster produced by the ionization particle. In case of minimum ionizing particles, such as cosmic rays, the optimal filter is a  $5 \times 5$  matrix. Hence, large spots formed by highly ionizing particles (such as helium and carbon at  $80\text{ MeV/n}$ ) almost vanish after filtration, blending into the background of the image. For highly ionizing particles, gathering large clusters of pixels, the optimized filter is a  $9 \times 9$  matrix.

In the FOOT experiment there are particles generating a wide ionization range, so the images acquired by microscope will undergo two different filtering processes. A  $9 \times 9$  filter will be used for emulsions with no thermal treatment to separate MIP from other ions. A  $5 \times 5$  filter will be adopted for emulsions with other thermal treatment. The merging of these two analyses, enables to estimate the ionization of each particle better.

The emulsions were exposed to cosmic rays from their production up to their chemical development (about one week). In order to minimize the integrated yield of cosmic rays, they were placed vertically during their storage and transportation. Signal and cosmic-rays can be distinguished thanks to their different angle tracks, since beam tracks have slopes below 0.2 while cosmic-ray tracks

extend well beyond. Denoting  $\theta_x$  and  $\theta_y$  the angular coordinates in the scanning system, signal tracks show  $\tan \theta < 0.2$  ( $\theta = \sqrt{\theta_x^2 + \theta_y^2}$ ), where  $\theta = 0$  corresponds to tracks perpendicular to the emulsion film.

## 4 Results

The tracks volume distribution obtained for films that did not undergo any thermal treatment (R0) is reported in Figure 4 for H,  $^2\text{H}$  and  $^{12}\text{C}$  beam (80 MeV/n), respectively.

Different entries in the plots reflect the different integrated

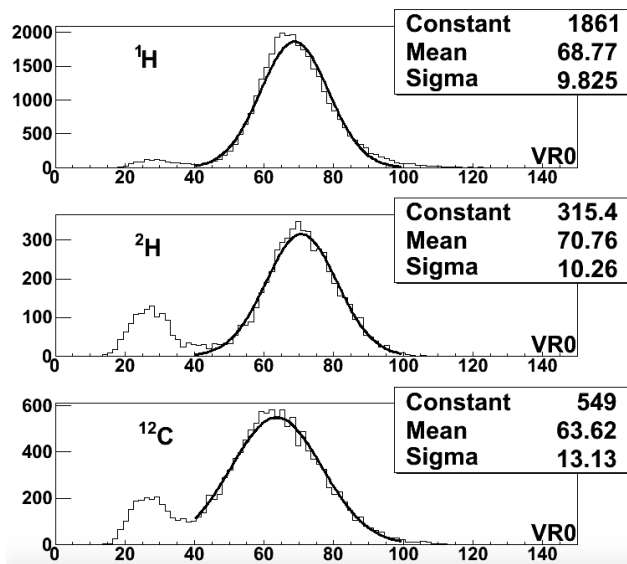


**Figure 4:** Track volume distribution for emulsions films that did not undergo any thermal treatment (R0) and were exposed at H,  $^2\text{H}$  and  $^{12}\text{C}$  beams (80 MeV/n) at LNS. The VR0 variable is measured in terms of number of pixels. The small peak on the left is due to the cosmic rays visible as MIP. The major peak is due to ion particles and a gaussian fit is superimposed to their experimental data.

fluxes. The distributions are obtained applying the angular cut at  $\tan\theta < 0.2$  to suppress the cosmic rays contribution. Anyway a small contamination of cosmic rays is still present, as visible in all the plots. The cosmic rays particles are at the minimum of their ionizing power (MIP) and they correspond to the small gaussian distribution (peak around  $\text{VR0} \sim 30$ ). The gaussian distribution at higher VR0 values is produced by ion particles. The values of the corresponding peaks do not allow any statistical separation ranging from protons to carbon.

The analysis of the emulsions underwent to the thermal treatment at  $28^\circ\text{C}$  (VR1) shows that H,  $^2\text{H}$  and MIP are completely erased, and only the tracks due to  $^4\text{He}$  and  $^{12}\text{C}$  parti-

cles are still present, as shown in Figure 5, where the track volume distributions for  $^4\text{He}$  and  $^{12}\text{C}$  particles are reported. The variable VR1 shows a clear separation between  $^4\text{He}$  and  $^{12}\text{C}$  with 5.3 standard deviations.

By analysing the plot in Figure 5, we quote the resolution on charge measurement for  $^4\text{He}$  and  $^{12}\text{C}$  to be about 5%. The scatter plot of VR1 vs VR2 is shown for  $^4\text{He}$  and  $^{12}\text{C}$  in

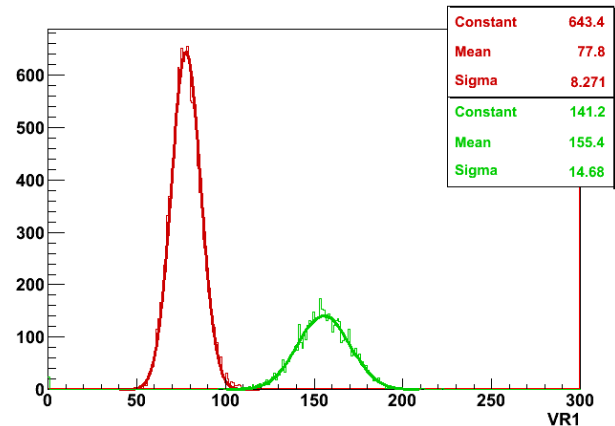


**Figure 5:** The distribution of  $^4\text{He}$  (red curve) and  $^{12}\text{C}$  (green curve) in terms of VR1 (corresponding to the number of pixels in the track volume).

Figure 6. We clearly see two populations, corresponding to the two different ions.

By projecting the distributions onto the axis passing

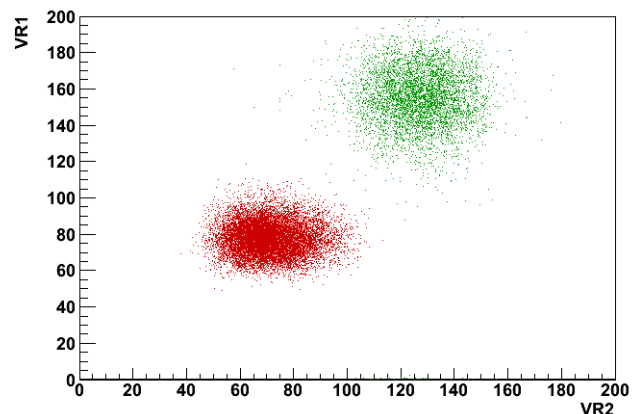


**Figure 6:** Scatter plot of VR1 versus VR2 for  $^4\text{He}$  (red) and  $^{12}\text{C}$  (green). The VR1 and VR2 variables are measured in terms of number of pixels.

through the two peak centres, the variable VR12 is obtained, as shown in Figure 7. By using this variable,  $^4\text{He}$  and  $^{12}\text{C}$  are separated with  $6.9 \sigma$  significance.

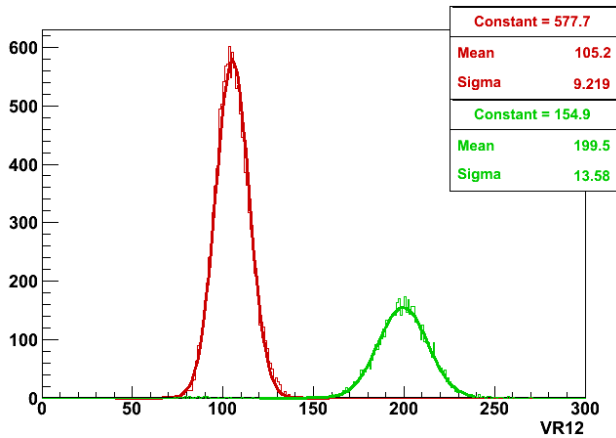


**Figure 7:** The distribution of  $^4\text{He}$  (red) and  $^{12}\text{C}$  (green) in terms of VR12.

Concerning the results obtained with higher temperature at  $36^\circ\text{C}$  and  $38^\circ\text{C}$ , corresponding respectively to R3 and R4 thermal treatments, a high erasing rate was observed determining a poor tracking efficiency. For this reason, the optimal temperature for the separation between  $^4\text{He}$  and  $^{12}\text{C}$  is  $34^\circ\text{C}$  was assessed.

## 5 Conclusions

We exposed twenty emulsion doublets to H,  $^2\text{H}$ ,  $^4\text{He}$  and  $^{12}\text{C}$  particles (80 MeV/n) at LNS. Emulsions underwent thermal treatments at different temperatures to achieve an optimal erasing rate for different ions with a new batch of emulsion films to be used for the spectrometer of the FOOT experiment.

By analysing the emulsions with newly developed fast scanning systems, particles according to their track volume by applying different thermal treatments were characterised. The films without any thermal treatment (R0) allow a separation better than  $3\sigma$  between MIP and ions (H,  $^2\text{H}$ ,  $^4\text{He}$  and  $^{12}\text{C}$ ). The low temperature refreshing treatment (R1) makes possible to separate H from  $^4\text{He}$  and  $^{12}\text{C}$  by erasing H tracks. Moreover the separation between  $^4\text{He}$  and  $^{12}\text{C}$  is also achieved, with  $5.3\sigma$  significance. A further increasing of the thermal treatment temperature (up to  $34^\circ\text{C}$ , R2 treatment) allows to improve the separation between  $^4\text{He}$  and  $^{12}\text{C}$  up to  $6.9\sigma$  significance.

The R2 thermal treatment is already sufficient to obtain a good separation between the different Z ions without excessive signal cancellation. Indeed, the authors decided not to use the thermal treatments at  $36^\circ\text{C}$  (R3) and  $38^\circ\text{C}$  (R4) causing a further erasing of the signal tracks without improving the ions separation. This result demonstrates

that the thermal treatment applied to this new batch of emulsion films allows extending their dynamical range and separating ions with high statistical significance. It is worth noting that the results reported in this work are obtained by a single layer emulsion detector, while the emulsion spectrometer of FOOT will use at least 9 films of each type. Therefore we expected to improve the resolution in the charge measurement and in the charge separation by a factor of 3. In the fragmentation studies of the FOOT experiment, lighter fragments will not be mono-energetic and the momentum spread will worsen the separation. These two effects partially compensate each other. Nevertheless, the separation achieved by the technique applied in this paper is certainly adequate to guarantee the performance required by the FOOT experiment.

**Acknowledgement:** We thank LNS for the successful operation in their facility during the data taking.

## References

- [1] Schardt D., Elsässer T., Schulz-Ertner D., Heavy-ion tumor therapy: Physical and radiobiological benefits, *Rev. Mod. Phys.*, 2010, 82, 383.
- [2] Paganetti H., Niemierko A, Ancukiewicz M., Gerweck L.E., Goitein M., Loeffler J.S. et al., Relative Biological Effectiveness (RBE) values for proton beam therapy, *Int. J. Radiation Oncology Biol. Phys.*, 2002, 53, 407-421.
- [3] Paganetti H., Relative Biological Effectiveness (RBE) values for proton beam therapy. Variations as a function of biological endpoint, dose, and linear energy transfer, *Phys. Med. Biol.*, 2014, 59, R419.
- [4] Carlsson C.A., Carlsson G.A., Proton dosimetry with 185 MeV protons. Dose buildup from secondary protons and recoil electrons, *Heath Phys.*, 1977, 33, 481-484.
- [5] Cucinotta F.A., Katz R., Wilson J.W., Townsend L.W., Shinn J. and Hajnal F., Biological effectiveness of high-energy protons: target fragmentation, *Radiat. Res.*, 1991, 127, 130-137.
- [6] Tommasino F., Durante M., *Proton Radiobiology*, *Cancer*, 2015, 7, 353.
- [7] FOOT Conceptual Design Report, <https://pandora.infn.it/public/912bb8> (accessed on 2018/01/11).
- [8] Morrocchi M., Ciarrocchi E., Alexandrov A., Alpat, B., Ambrosi G, Argirò et al., Development and characterization of a  $\Delta E - \text{TOF}$  detector prototype for the FOOT experiment, *NIM A*, 2018, 916, 116.
- [9] De Lellis G., Buontempo S., Di Capua F., Marotta A., Migliozi P., Petukhov Y. et al., Emulsion Cloud Chamber technique to measure the fragmentation of high-energy carbon beam, *J. Instrum*, 2007, 2, P06004.
- [10] De Lellis G., Buontempo S., Di Capua F., Di Crescenzo A., Migliozi P., Petukhov Y. et al., Measurements of the fragmentation of carbon nuclei used in hadron therapy, *Nuclear Physics A*, 2011, 853, 124.

- [11] Nakamura T. et al., The OPERA film: new nuclear emulsion for large-scale, high-precision experiments, *NIM A*, 2006, 556, 80.
- [12] Alexandrov A., De Lellis G., Di Crescenzo A., Lauria A., Montesi M.C., Pastore A. et al., Measurement of  $^{12}\text{C}$  ions beam fragmentation at large angle with an Emulsion Cloud Chamber, *J. Instrum.*, 2017, 11, P08013.
- [13] Alexandrov A., Bozza C., Buonaura A., Consiglio L., D'Ambrosio N., De Lellis G. et al., Improving the detection efficiency in nuclear emulsion trackers, *NIM A*, 2015, 776, 45.
- [14] Alexandrov A., Buonaura A., Consiglio L., D'Ambrosio N., De Lellis G., Di Crescenzo A. et al., A new fast scanning system for the measurement of large angle tracks in nuclear emulsions, *J. Instrum.*, 2015, 10, P11006.
- [15] Alexandrov A., Buonaura A., Consiglio L., D'Ambrosio N., De Lellis G., Di Crescenzo A. et al., A new generation scanning system for the high-speed analysis of nuclear emulsions, *J. Instrum.*, 2016, 11, P06002.
- [16] Arrabito L., Bozza C., Buontempo S., Consiglio L., Cozzi M., D'Ambrosio N. et al. Track reconstruction in the emulsion-lead target of the OPERA experiment using the ESS microscope, *J. Instrum.*, 2017, 2, P05004.
- [17] Alexandrov A., Buonaura A., Consiglio L., D'Ambrosio N., De Lellis G., Di Crescenzo A. et al., The continuous motion technique for a new generation of scanning systems, *Scientific reports*, 2017, 7, 7310.
- [18] Tommasino F., Rovituro M., Fabiano S., Pier S., Manea C., Lorentini S. et al., Proton beam characterization in the experimental room of the Trento Proton Therapy facility, *Nuclear Instruments and Methods in Physics Research Section A: Accelerators, Spectrometers, Detectors and Associated Equipment*, 2017, 869, 15-20.
- [19] Aleksandrov A., Polukhina N.G. and Starkov N.I. *Methods for Image Recognition of Charged Particle Tracks in Track Detector Data Automated Processing*, Astrophysics, Prof. Ibrahim Kucuk (Ed.), ISBN: 978-953-51-0473-5, InTech., 2012.
- [20] Nakamura T. et al., The OPERA film: new nuclear emulsion for large scale, high precision experiments, *Nucl. Instrum. Meth. B*, 1996, 117, 221.